

Nonadiabatic couplings from the Kohn-Sham derivative matrix: Formulation by time-dependent density-functional theory and evaluation in the pseudopotential framework

Chunping Hu,^{1,*} Osamu Sugino,² Hirotohi Hirai,² and Yoshitaka Tateyama^{1,3}

¹WPI International Center for Materials Nanoarchitectonics, National Institute for Materials Science, Tsukuba, Ibaraki 305-0044, Japan

²Institute for Solid State Physics, University of Tokyo, Kashiwa, Chiba 277-8581, Japan

³PRESTO and CREST, Japan Science and Technology Agency, 4-1-8 Honcho, Kawaguchi, Saitama 332-0012, Japan

(Received 8 October 2010; published 10 December 2010)

We study the time-dependent density-functional theory formulation of nonadiabatic couplings (NAC's) to settle problems regarding practical calculations. NAC's have so far been rigorously formulated on the basis of the density response scheme and expressed using the nuclear derivative of the Hamiltonian, $\partial H/\partial R$, whereby causing the pseudopotential problem. When rewritten using the nuclear derivative operator, $\partial/\partial R$, or the d operator, the formula is found free of the problem and thus provides a working numerical scheme. The d -operator-based formulation also allows us to lay a foundation on the empirical Slater transition-state method and to show an improved way of using the auxiliary excited-state wave-function ansatz, both of which have been utilized in previous works. Evaluation of NAC near either the Jahn-Teller or the Renner-Teller intersection in various molecular systems shows that the values of NAC are much improved over previous calculations when the d -operator formula is implemented in the pseudopotential framework.

DOI: [10.1103/PhysRevA.82.062508](https://doi.org/10.1103/PhysRevA.82.062508)

PACS number(s): 31.15.ee, 31.10.+z, 31.50.Gh

I. INTRODUCTION

Electronic degeneracy commonly exists in polyatomic systems. Owing to the Jahn-Teller theorem [1,2] that the ground state will be free of degeneracy to the greatest extent possible, the equilibrium properties can usually be described conveniently using the adiabatic (Born-Oppenheimer) approximation to separate the nuclear and electronic degrees of freedom. When dynamical properties are concerned, however, the system can approach the degeneracy point where the adiabatic approximation is no longer valid [3–5]. The nonadiabatic coupling (NAC), a driving force for nonadiabatic transition to different potential energy surfaces (PES's) [6,7], is infinity at the degeneracy point and nonnegligible in that vicinity, indicating that the NAC is as important as the PES in determining the dynamical properties near the degeneracy point [8–11]. Although the adiabatic-to-diabatic transformation [3,4,12,13] may be used to partially remove the NAC in the formulation [14,15], the residual NAC is not necessarily negligible, which means that explicit evaluation of the NAC is critically important for the understanding of nonadiabatic processes.

To calculate the NAC, wave-function-based methods were predominantly used in the past, but their computational cost grows too rapidly with the system size. In the past decade, on the other hand, density response methods have been developed within the time-dependent density-functional theory (TDDFT), showing great promise in resolving the cost problem. The study was initiated by Chernyak and Mukamel [16], who proposed to perturb the ground state using a nuclear derivative of the Hamiltonian, $\partial H/\partial R_\mu$, multiplied by a monochromatic oscillating coefficient, $e^{i\omega t}$, whereby the spectral function of the linear susceptibility (or dynamic

polarizability) is proportional to the square of the NAC. Then, one can obtain the NAC, except for the phase factor, by calculating the susceptibility within the TDDFT and taking its residue. This scheme was first implemented to a plane-wave (PW) code by Baer [17] to study H₃ using a real-time approach and then to a PW-pseudopotential (PP) code by Hu *et al.* [18,19] to systematically study small molecules using a frequency domain approach from Casida [20,21]. It was revealed that NAC's thus obtained are in reasonable agreement with those obtained by theoretical models or correlated wave-function methods for both Jahn-Teller [1] and Renner-Teller [22] types of intersections in spite of using the adiabatic local density approximation (ALDA). The modified linear response scheme [23,24] allows successful application of the scheme quite close to the degeneracy points. However, good agreement was achieved only for monovalent elements; for other elements, the results were not only unsatisfactory but also quite sensitively dependent on PP's [19]. This PP problem can be traced back to inaccurate description of the off-diagonal elements of $\partial H/\partial R_\mu$, such as that between $2s$ and $2p$ of an atom, which is usually not guaranteed in the PP framework. Note that such off-diagonal scattering terms, which may also be called inelastic scattering terms, do not appear in the ground-state calculations but do appear in the NAC calculation. Hu *et al.* [25] showed that the value of the NAC is much improved when using an all-electron linear combination of atomic orbitals (LCAO) scheme formulated following Tommasini *et al.* [26], and concluded that PP, rather than ALDA, is indeed the major source of error. Here we show that the PP problem can be eliminated by using the d -matrix [or the Kohn-Sham (KS) matrix element for the nuclear derivative operator, $\langle \psi_{i\sigma} | \frac{\partial \hat{H}}{\partial R_\mu} | \psi_{j\sigma} \rangle$] representation of NAC instead of the h -matrix (or the KS matrix element for the operator $\partial H/\partial R_\mu$, $\langle \psi_{i\sigma} | \frac{\partial \hat{H}}{\partial R_\mu} | \psi_{j\sigma} \rangle$) representation which is given in Refs. [18] and [19]. This is because the d matrix can be safely calculated with PP in contrast to the h matrix. In the following we provide the d -matrix-based formula of the

*Present address: Department of Physics, Tokyo University of Science, 1-3 Kagurazaka, Shinjuku, Tokyo 162-8601, Japan; hu@rs.kagu.tus.ac.jp

NAC and show that numerical results can be much improved over previous calculations based on the h -matrix formula.

The other aim of this paper is to clarify the similarity and difference between existing d -matrix formulations for the NAC [8,9,27,28]. The d -matrix was previously recognized as the ‘‘NAC between KS orbitals’’ [29] and used for NAC simply assuming a single-electron picture of static density-functional theory to be valid at excited states as well [30–32]. Despite the lack of justification, Billeter and Curioni [27] showed that the mere d -matrix element between the particle and the hole in the Slater transition state is particularly accurate for the demonstrated systems. We will show that our d -matrix formula can justify this intuitive approach when combined with the modified linear response theory, not only for the equilibrium geometries as demonstrated in Ref. [27] but also in the very vicinity of either Jahn-Teller or Renner-Teller types of intersections. More recently, d -matrix formulation was derived in the work of Tavernelli *et al.* [8,9,28] on the basis of the Casida ansatz with the use of the auxiliary wave function, which is an effective wave function to reproduce the density response of a system perturbed with a time-dependent local field. This approach was first presented without much justification [8]; however, comparison of NAC values with complete active space self-consistent field (CASSCF) calculations shows that it is promising to give reasonably good results for demonstrated systems. Later the validation of this approach was given [33] in a way in which the d operator is used as a local field to give the perturbation to the electrons, although such a perturbation cannot be usually described by the d operator. Here we will show that using our present d -matrix formula, the good performance of the Casida ansatz in demonstrated systems can be easily understood, although the rigorous formula shows that the Casida ansatz in constructing auxiliary wave functions needs to be modified for the general purpose of calculating NAC, which might be important for future applications.

The present paper is organized as follows: In Sec. II, we present the formulation of the NAC free of the PP problem, starting from our established formula of the NAC. Therein we discuss the connection of our formula to other existing formulations. Justification of the Slater transition-state method will be also made. In Sec. III, implementation in the PW-PP framework and computational details are given. In Sec. IV, practical calculations on various molecular systems possessing Jahn-Teller or Renner-Teller intersections are performed and compared with models or *ab initio* results in the literature. In Sec. V, we conclude our work.

II. FORMULATION

The density response scheme of Hu *et al.* [18] begins by relating the sum-over-state representation of the dynamic polarizability

$$\alpha_{\mu\nu}(\omega) = \sum_I \frac{2\omega_I \langle \Psi_0 | \frac{\partial \hat{H}}{\partial R_\mu} | \Psi_I \rangle \langle \Psi_I | \frac{\partial \hat{H}}{\partial R_\nu} | \Psi_0 \rangle}{\omega_I^2 - \omega^2} \quad (1)$$

for a system perturbed by

$$\frac{\partial \hat{H}}{\partial R_\mu} (e^{i\omega t} + e^{-i\omega t}) = \frac{\partial \hat{V}^{e,n}}{\partial R_\mu} (e^{i\omega t} + e^{-i\omega t}) \quad (2)$$

with the Casida formalism [20] of the same quantity

$$\alpha_{\mu\nu}(\omega) = \sum_I \frac{2\mathbf{h}_\mu^\dagger \mathbf{S}^{-1/2} \mathbf{F}_I \mathbf{F}_I^\dagger \mathbf{S}^{-1/2} \mathbf{h}_\nu}{\omega_I^2 - \omega^2} \quad (3)$$

to yield NAC as

$$\langle \Psi_0 | \frac{\partial}{\partial R_\mu} | \Psi_I \rangle = \omega_I^{-1} \langle \Psi_0 | \frac{\partial \hat{H}}{\partial R_\mu} | \Psi_I \rangle = \omega_I^{-3/2} \mathbf{h}_\mu^\dagger \mathbf{S}^{-1/2} \mathbf{F}_I. \quad (4)$$

Here Ψ_0 (Ψ_I) is the many-body electronic wave function of the ground (I th excited) state, R_μ is the nuclear coordinate with μ representing x , y , and z components and the atom index, \hat{H} is the many-body Hamiltonian, $\hat{V}^{e,n}$ is the potential from the nuclear charge, and ω_I is the excitation energy. Matrix elements of \mathbf{S} and \mathbf{h}_μ are given by

$$S_{ij\sigma,kl\tau} = \frac{\delta_{\sigma,\tau} \delta_{i,k} \delta_{j,l}}{(f_{k\tau} - f_{l\tau})(\varepsilon_{l\tau} - \varepsilon_{k\tau})} \quad (5)$$

and

$$h_{\mu,ij\sigma} = \langle \psi_{i\sigma} | \frac{\partial \hat{H}}{\partial R_\mu} | \psi_{j\sigma} \rangle, \quad (6)$$

where $\psi_{i\sigma}$, $\varepsilon_{i\sigma}$, and $f_{i\sigma}$ are, respectively, the orbital, eigenvalue, and occupation number for the i th KS state with spin σ . \mathbf{F}_I is the eigenvector of the Casida equation [20]

$$\Omega \mathbf{F}_I = \omega_I^2 \mathbf{F}_I, \quad (7)$$

where

$$\begin{aligned} \Omega_{ij\sigma,kl\tau} &= \delta_{\sigma,\tau} \delta_{i,k} \delta_{j,l} (\varepsilon_{l\tau} - \varepsilon_{k\tau})^2 \\ &\quad + 2\sqrt{(f_{i\sigma} - f_{j\sigma})(\varepsilon_{j\sigma} - \varepsilon_{i\sigma})} K_{ij\sigma,kl\tau} \\ &\quad \times \sqrt{(f_{k\tau} - f_{l\tau})(\varepsilon_{l\tau} - \varepsilon_{k\tau})}, \end{aligned} \quad (8)$$

with \mathbf{K} being the KS matrix of the Hartree and exchange-correlation (xc) kernel (Λ^{Hxc}),

$$\begin{aligned} K_{ij\sigma,kl\tau} &= \iint d\mathbf{r} d\mathbf{r}' \overline{\psi_{i\sigma}(\mathbf{r}) \psi_{j\sigma}(\mathbf{r})} \\ &\quad \times \Lambda^{\text{Hxc}}(\mathbf{r}, \mathbf{r}') \psi_{k\tau}(\mathbf{r}') \psi_{l\tau}(\mathbf{r}'). \end{aligned} \quad (9)$$

In this paper, we assume the KS orbitals to be real for simplicity.

A. The d -matrix representation

So far NAC has been expressed using the h matrix [Eq. (6)], as in Eq. (4). Next we show that it can also be expressed using the d matrix,

$$d_{\mu,ij\sigma} \equiv \langle \psi_{i\sigma} | \frac{\partial}{\partial R_\mu} | \psi_{j\sigma} \rangle, \quad (10)$$

which can be rewritten either by the derivative of the KS Hamiltonian or by the derivative of the effective KS potential as

$$d_{\mu,ij\sigma} = \frac{\langle \psi_{i\sigma} | \frac{\partial \hat{H}^{\text{KS}}}{\partial R_\mu} | \psi_{j\sigma} \rangle}{\varepsilon_{j\sigma} - \varepsilon_{i\sigma}} = \frac{\langle \psi_{i\sigma} | \frac{\partial \hat{V}^{\text{eff}}}{\partial R_\mu} | \psi_{j\sigma} \rangle}{\varepsilon_{j\sigma} - \varepsilon_{i\sigma}}, \quad (11)$$

where \hat{V}^{eff} is given as $\hat{V}^{\text{eff}} = \hat{V}^{e,n} + \hat{V}^{\text{Hxc}}$ and \hat{V}^{Hxc} is the Hartree exchange correlation potential. It is straightforward to relate the h matrix to the d matrix via the formula

$$\begin{aligned} \frac{\partial V^{\text{eff}}(\mathbf{r})}{\partial R_\mu} &= \frac{\partial V^{e,n}(\mathbf{r})}{\partial R_\mu} + \int d\mathbf{r}' \frac{\delta V^{\text{Hxc}}(\mathbf{r})}{\delta \rho(\mathbf{r}')} \frac{\partial \rho(\mathbf{r}')}{\partial R_\mu} \\ &= \frac{\partial V^{e,n}(\mathbf{r})}{\partial R_\mu} + \int d\mathbf{r}' \Lambda^{\text{Hxc}}(\mathbf{r}, \mathbf{r}') \\ &\quad \times \int d\mathbf{r}'' \frac{\delta \rho(\mathbf{r}'')}{\delta V_{\text{eff}}(\mathbf{r}'')} \frac{\partial V^{\text{eff}}(\mathbf{r}'')}{\partial R_\mu} \\ &= \frac{\partial V^{e,n}(\mathbf{r})}{\partial R_\mu} + \int \int d\mathbf{r}' d\mathbf{r}'' \Lambda^{\text{Hxc}}(\mathbf{r}, \mathbf{r}') \\ &\quad \times \chi^{\text{KS}}(\mathbf{r}', \mathbf{r}'') \frac{\partial V^{\text{eff}}(\mathbf{r}'')}{\partial R_\mu}. \end{aligned} \quad (12)$$

Herein χ^{KS} is the KS density response function [34,35]

$$\begin{aligned} \chi^{\text{KS}}(\mathbf{r}, \mathbf{r}') &= \frac{\delta \rho(\mathbf{r})}{\delta V_{\text{eff}}(\mathbf{r}')} \\ &= -2 \sum_{kl\tau}^{f_{k\tau} > f_{l\tau}} \frac{f_{k\tau} - f_{l\tau}}{\epsilon_{l\tau} - \epsilon_{k\tau}} \psi_{k\tau}(\mathbf{r}) \\ &\quad \times \psi_{k\tau}(\mathbf{r}') \psi_{l\tau}(\mathbf{r}) \psi_{l\tau}(\mathbf{r}'). \end{aligned} \quad (13)$$

By taking the KS matrix element of Eq. (12), we get

$$\begin{aligned} (\epsilon_{i\sigma} - \epsilon_{j\sigma}) d_{\mu,ij\sigma} &= h_{\mu,ij\sigma} - \sum_{kl\tau}^{f_{k\tau} > f_{l\tau}} 2(f_{k\tau} - f_{l\tau}) K_{ij\sigma,kl\tau} d_{\mu,kl\tau}, \end{aligned} \quad (14)$$

which can be further transformed as

$$\begin{aligned} h_{\mu,ij\sigma} &= \sum_{kl\tau}^{f_{k\tau} > f_{l\tau}} [(\epsilon_{j\sigma} - \epsilon_{i\sigma}) \delta_{i,k} \delta_{j,l} \delta_{\sigma,\tau} + 2(f_{k\tau} - f_{l\tau}) K_{ij\sigma,kl\tau}] \\ &\quad \times d_{\mu,kl\tau}. \end{aligned} \quad (15)$$

This is the central equation which relates the h matrix to the d matrix. Using the Casida equation [Eq. (7)] we can rewrite Eq. (4) as

$$\langle \Psi_0 | \frac{\partial}{\partial R_\mu} | \Psi_I \rangle = \omega_I^{-1/2} \mathbf{d}_\mu^\dagger \mathbf{S}^{1/2} \mathbf{F}_I \quad (16)$$

from the relationship

$$\begin{aligned} \mathbf{F}_I^\dagger \mathbf{S}^{-1/2} \mathbf{h}_\mu &= \sum_{ij\sigma}^{f_{i\sigma} > f_{j\sigma}} F_I^{ij\sigma} \sqrt{(f_{i\sigma} - f_{j\sigma}) (\epsilon_{j\sigma} - \epsilon_{i\sigma})} h_{\mu,ij\sigma} \\ &= \sum_{ij\sigma}^{f_{i\sigma} > f_{j\sigma}} \sum_{kl\tau}^{f_{k\tau} > f_{l\tau}} F_I^{ij\sigma} \Omega_{ij\sigma,kl\tau} \\ &\quad \times \frac{\delta_{\sigma,\tau} \delta_{i,k} \delta_{j,l}}{\sqrt{(f_{k\tau} - f_{l\tau}) (\epsilon_{l\tau} - \epsilon_{k\tau})}} (f_{k\tau} - f_{l\tau}) d_{\mu,kl\tau} \\ &= \mathbf{F}_I^\dagger \Omega \mathbf{S}^{1/2} \mathbf{d}_\mu = \mathbf{F}_I^\dagger \omega_I^2 \mathbf{S}^{1/2} \mathbf{d}_\mu, \end{aligned} \quad (17)$$

where $f_{i\sigma} - f_{j\sigma} = 1$ is used. The alternative formulation of the NAC by Eq. (16) avoids the explicit evaluation of the

h matrix and is free from the PP problem as shown in the following.

Equation (16) can be further used to analyze the formulation of Tavernelli *et al.* [8,36] using the Casida ansatz [20] that the wave function of a system perturbed by a monochromatic oscillating one-body operator \hat{O} , or a monochromatic oscillating local field operator, is effectively described by the auxiliary wave function

$$\tilde{\Psi}_I = \sum_{ij\sigma}^{f_{i\sigma} > f_{j\sigma}} \sqrt{\frac{\omega_I - \epsilon_{i\sigma}}{\omega_I}} F_{ij\sigma,I} \hat{a}_{j\sigma}^\dagger \hat{a}_{i\sigma} \tilde{\Psi}_0 \quad (18)$$

so that $\langle \tilde{\Psi}_0 | \hat{O} | \tilde{\Psi}_I \rangle$ is equal to the one obtained using the Casida formalism. Herein $\hat{a}_{i\sigma}^\dagger$ ($\hat{a}_{i\sigma}$) is the creation (annihilation) operator and $\tilde{\Psi}_0$ is the Slater determinant of the static KS eigenstates. Tavernelli *et al.* [8,36] used it to get the NAC as

$$\langle \tilde{\Psi}_0 | \frac{\partial}{\partial R_\mu} | \tilde{\Psi}_I \rangle = \omega_I^{-1/2} \mathbf{d}_\mu^\dagger \mathbf{S}^{-1/2} \mathbf{F}_I. \quad (19)$$

This formulation is based on general linear response theory, where the one-body operator directly couples with the electron density as a local field $V(\mathbf{r})$. However, the d operator ($\partial/\partial R_\mu$) is not such a one-body operator like the h operator ($\partial \hat{H} / \partial R_\mu$) because it cannot be represented as the local field, and therefore the linear response theory cannot be straightforwardly applied. This means that the Casida ansatz cannot be straightforwardly applied when the d operator is concerned and the d -matrix formulation needs to be derived in a distinct way (we have done it via the h -matrix formulation). The difference between two d -matrix formulations, that is, Eqs. (19) and (16) (the rigorous one), however, is seen only in the power of \mathbf{S} and ω_I , so the reasonably good performance of the auxiliary wave-function approach for demonstrated systems can be easily understood, as reported in a series of publications of Tavernelli *et al.* On the other hand, for future applications to more general systems, it is necessary to construct the auxiliary wave function in an improved way as

$$\tilde{\Psi}_I = \sum_{ij\sigma}^{f_{i\sigma} > f_{j\sigma}} \sqrt{\frac{\omega_I}{\epsilon_{j\sigma} - \epsilon_{i\sigma}}} F_{ij\sigma,I} \hat{a}_{j\sigma}^\dagger \hat{a}_{i\sigma} \tilde{\Psi}_0. \quad (20)$$

With such a ‘‘subtle’’ modification, the auxiliary approach would be equivalent to our formula of Eq. (16). It is noted that the applicability of the adapted ansatz in Eq. (20) also depends on which operator \hat{O} is used: It is suitable for the d operator, but not for the h operator or the dipole operator. For the latter cases, the Casida ansatz in Eq. (18) should be used, as proven by Tavernelli *et al.* [36].

B. Good performance of the Slater transition-state method: Justification by TDDFT modified linear response theory

Different from the previously mentioned TDDFT formulation, a simple procedure in which single d -matrix elements are just assumed as NAC, has been seen in previous studies and the results on nonadiabatic dynamics are promising for the demonstrated system [30–32]. This can be understood from a simple analysis of the relationship between the NAC and the d matrix, as shown by Eq. (16): When there is

a dominant transition and the excitation energy is close to the eigenenergy difference of the orbitals responsible for the transition, the single d -matrix element corresponding to the dominant transition will be a good representation of NAC. A particular example is the case of the Slater transition-state method for doublet systems. Billeter and Curioni [27] have used the following expression of NAC:

$$\langle \Psi_0 | \hat{d}_\mu | \Psi_I \rangle = \langle \psi_{i\sigma}^m | \hat{d}_\mu | \psi_{j\sigma}^m \rangle, \quad (21)$$

where the (i, j) pair are the particle-hole orbitals responsible for the I th transition, and m denotes the mid-excited state (Slater transition state) in which the particle-hole orbitals are each filled with a half-electron. They have found that this expression can give accurate results of NAC between doublet states of molecules at equilibrium geometries.

Next we will show that the extension of TDDFT formulation of the NAC from the d matrix within modified linear response theory [23,24], which has been demonstrated to be a better way to decode excitation energies by TDDFT from local density approximation, can give justification of the good performance of the Slater transition-state method. Within modified linear response, the excitation energy is calculated from the response of the mid-excited state, while other terms in the NAC formula are calculated from that of the pure-state configuration. Corresponding to the mid-excited state of a doublet system, the Casida equation,

$$\Omega^m \mathbf{F}_I^m = \omega_I^m \mathbf{F}_I^m, \quad (22)$$

with the matrix element

$$\begin{aligned} \Omega_{ij\sigma,kl\tau}^m &= \delta_{i,k} \delta_{j,l} \delta_{\sigma,\tau} (\epsilon_{j\sigma}^m - \epsilon_{i\sigma}^m)^2 \\ &+ 2(f_{i\sigma}^m - f_{j\sigma}^m) (\epsilon_{j\sigma}^m - \epsilon_{i\sigma}^m) K_{ij\sigma,kl\tau}^m, \end{aligned} \quad (23)$$

gives

$$\omega_I^m = \epsilon_{j\sigma}^m - \epsilon_{i\sigma}^m, \quad (24)$$

since $f_{i\sigma}^m = f_{j\sigma}^m = 0.5$ in the mid-excited state of a doublet system, which renders the corresponding off-diagonal elements of Ω to be zero. On the other hand, the pure-state configuration in the mid-excited state, which uses the occupation number of the

ground state while keeping other quantities of the mid-excited state, gives

$$\mathbf{d}_{\mu,p}^\dagger \mathbf{S}_p^{1/2} \mathbf{F}_I^p = d_{ij\sigma}^m (\epsilon_{j\sigma}^m - \epsilon_{i\sigma}^m)^{-1/2}, \quad (25)$$

due to the fact that $F_{ij\sigma,I}^p$ is practically equivalent to 1 and other components of \mathbf{F}_I^p are zero. Therefore,

$$\langle \Psi_0 | \hat{d}_\mu | \Psi_I \rangle = (\omega_I^m)^{1/2} \mathbf{d}_{\mu,p}^\dagger \mathbf{S}_p^{1/2} \mathbf{F}_I^p = d_{ij\sigma}^m, \quad (26)$$

which is just the expression used by Billeter and Curioni [27]. The good performance of this expression in the computation of the NAC between the ground and excited states of doublet systems can thus be understood from the fact that it is the reduced form of the TDDFT formulation.

III. IMPLEMENTATION AND COMPUTATIONAL DETAILS

The implementation of the present TDDFT method of computing the NAC from the d matrix is based on the ABINIT code [37], which is a PW-PP approach. All calculations are performed within ALDA or local spin density approximation using the Teter Pade parametrization [38]. The Troullier-Martins PP's [39] with nonlinear core correction [40], generated by Khein and Allan, as well as Hartwigsen-Goedecker-Hutter (HGH) PP's [41], are used for various atomic species. Only the Γ point ($k = 0$) is taken into consideration in the \mathbf{k} point sampling, which corresponds to the use of real wave functions. Convergence parameters, such as the supercell size, number of unoccupied orbitals, and kinetic energy cutoff, are examined to ensure reasonably accurate results. On the basis of the previous implementation of modified linear response theory in ABINIT [24], its extension for calculating NAC requires almost no additional labor, since it is only necessary to construct the pure-state configuration from the mid-excited state, and to apply the same calculation procedures as ordinary linear response theory. To check the performance of our method, we concentrate on NAC between the ground and first excited state in Jahn-Teller and Renner-Teller systems.

A. Finite difference method of calculating d -matrix elements

The calculation of the d matrix is implemented in a straightforward finite difference scheme, with the consideration of aligning the phases of KS orbitals [27], as shown by

$$\langle \psi_{i\sigma} | \hat{d}_\mu | \psi_{j\sigma} \rangle = \frac{\langle \psi_{i\sigma}(\mathbf{R}) | \psi_{j\sigma}(\mathbf{R} + \frac{1}{2} \Delta R \mathbf{e}_\mu) \text{sgn}(\xi_+) - \psi_{j\sigma}(\mathbf{R} - \frac{1}{2} \Delta R \mathbf{e}_\mu) \text{sgn}(\xi_-) \rangle}{\Delta R}, \quad (27)$$

where \mathbf{e}_μ is the unit vector along the μ axis, $\text{sgn}(\xi)$ is the sign function, that is,

$$\text{sgn}(\xi) = \begin{cases} -1 & \text{if } \xi < 0 \\ 1 & \text{if } \xi > 0, \end{cases} \quad (28)$$

and

$$\xi_+ = \langle \psi_{j\sigma}(\mathbf{R}) | \psi_{j\sigma}(\mathbf{R} + \frac{1}{2} \Delta R \mathbf{e}_\mu) \rangle, \quad (29)$$

$$\xi_- = \langle \psi_{j\sigma}(\mathbf{R}) | \psi_{j\sigma}(\mathbf{R} - \frac{1}{2} \Delta R \mathbf{e}_\mu) \rangle. \quad (30)$$

In practical calculations we choose $\Delta R = 0.001$ bohr. Note that the finite difference method might be cumbersome for large systems and analytical schemes such as the one presented by Billeter and Curioni [27] are desired in the implementation; however, due to the simplicity of the finite difference method it is adopted here for the test calculation of small molecular systems.

IV. RESULTS AND DISCUSSION

In this section, we present calculation results on various molecular systems possessing Jahn-Teller or Renner-Teller intersections, for which the NAC between the ground and the first excited state is significant in the vicinity of intersection points.

A. Performance of TDDFT linear response theory on the computation of NAC from d -matrix elements

To examine the performance of TDDFT linear response theory, we choose molecular geometries in the reasonable vicinity of intersection points, where the values of NAC are significant and ordinary linear response theory is also applicable, as demonstrated in our previous work [18].

1. Jahn-Teller systems

For the computation of NAC, the H_3 system is most widely studied by various theoretical approaches [17,42–45]. We first focus on this prototype Jahn-Teller system to evaluate the performance of our present TDDFT scheme by comparing it with the multiconfiguration self-consistent-field configuration-interaction (MCSCF CI) data [46], as well as the one based on the Casida ansatz. The calculation geometry of H_3 is represented in the hyperspherical coordinate (ρ, θ, ϕ) while fixing $\rho = 2.5$ bohr and $\phi = 120^\circ$. According to the fact that the smaller the hyperspherical angle θ is, the closer the system is to the conical intersection ($\theta = 0^\circ$), we decrease θ from 10° to 1° in the calculations. In such a range of θ , the TDDFT LDA results of our previous PP calculation [18] using the h matrix are shown to be in reasonable agreement with the reference data. In Fig. 1, it is seen that the present TDDFT method which rigorously formulates the NAC from the d matrix gives similar but obviously improved results in comparison to the TDDFT scheme based on the Casida ansatz. Compared with the reference data of MCSCF CI calculations [46], our result shows reasonable agreement for $\theta > 1^\circ$, but rapidly deteriorates as θ approaches 1° . This behavior is anticipated since the performance of the TDDFT LDA degrades when approaching the very vicinity of the intersection point. In our previous TDDFT calculation using the h matrix, a similar trend is seen except for $\theta = 1^\circ$, where the previous calculation shows better agreement. We infer that this difference might be attributed to the pseudization of the \hat{h}_μ operator as the nuclear derivative of PP's, which might suppress the diverging behavior of the NAC when approaching intersection points.

It is known that Jahn-Teller systems show quantized behavior of angular NAC on a contour around the intersection point [45,47]. Usually the angular NAC will oscillate since the ideal value (0.5) predicted by the Jahn-Teller model is limited to an infinitely small region surrounding the intersection point. To check this feature we set H_3 in the geometry of Fig. 2 and choose the distance $R_{H-H} = 1.044$ Å and the contour radius $q = 0.3$ Å as used by Halašz *et al.* [44]. When the contour angle φ is varied from 0° to 360° , it is seen that the angular NAC of H_3 is in an oscillation around 0.5, as shown in Fig. 3. Our TDDFT results are in reasonable agreement with the reference data calculated at the CASSCF level [44], as previously confirmed by our calculation based on the TDDFT formulation of the

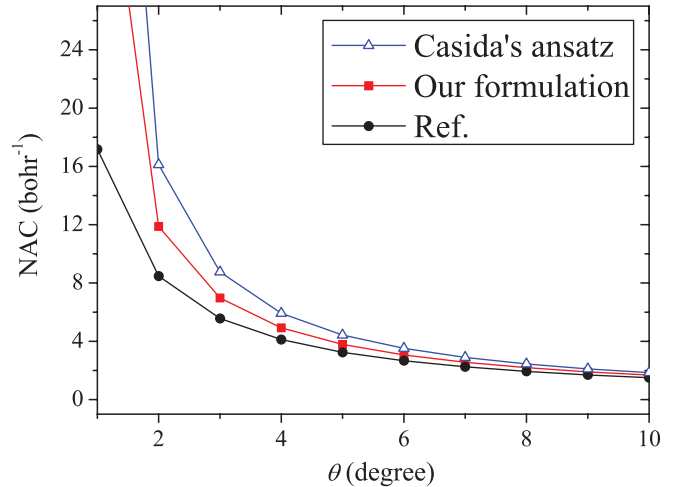


FIG. 1. (Color online) The x components of NAC on the second H atom of H_3 as a function of the hyperspherical angle θ , computed by different methods: our TDDFT method using the d matrix (filled squares), the TDDFT method based on the Casida ansatz (open triangles), as well as the MCSCF CI method by Abrol *et al.* [46] (filled circles).

h matrix [18]. A further look at two metal trimers, Li_3 and Na_3 (Table I), which are also well-known Jahn-Teller systems, shows that similar behavior of fluctuation around 0.5 in angular NAC (equal to the product of the component on the rotating atom and the contour radius q when φ is 0) is observed. Due to the PP approximation in constructing h -matrix elements, the TDDFT calculation using the d matrix gives slightly better results in the sense that it shows better accuracy in the satisfaction of the sum rule [26], which states that the sum of NAC components on all atoms, either in the x , y , or z direction, should be zero according to translational invariance.

2. Renner-Teller systems

The triatomic molecules, BH_2 , NH_2 , CH_2^+ , and H_2O^+ , which are typical Renner-Teller systems possessing glancing intersections between ground and first excited states [47–51], are used in the calculations. Similar to Jahn-Teller systems,

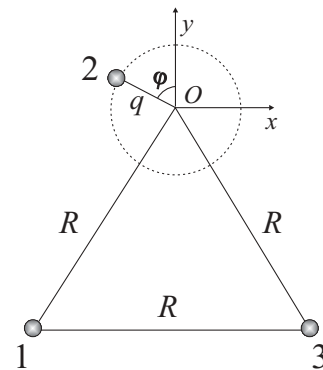


FIG. 2. The geometry of the X_3 system as one X atom (numbered as 2) is moved on the contour around the intersection point (located at O). The nuclear configuration at the intersection point is an equilateral triangle with C_{3v} symmetry, corresponding to the degeneracy of the ground state and the first excited state.

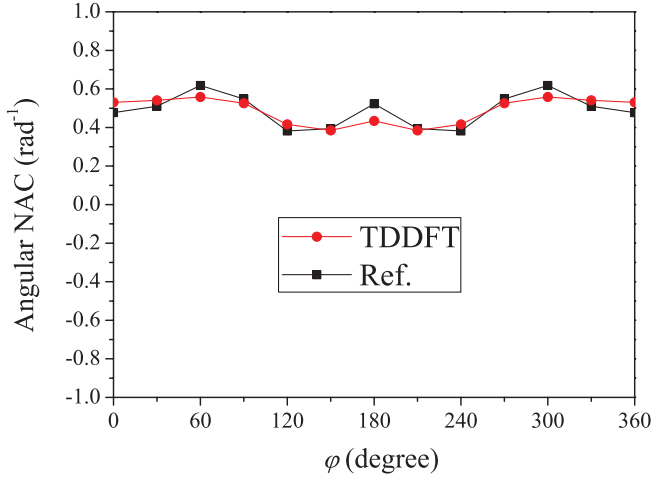


FIG. 3. (Color online) The angular NAC of the H_3 system ($R_{H-H} = 1.044 \text{ \AA}$ and $q = 0.3 \text{ \AA}$ in Fig. 2) as a function of φ , calculated by the present TDDFT linear response scheme using the d matrix (filled circles). The reference data [44] are shown by filled squares.

Renner-Teller systems also show quantized behavior of angular NAC with the ideal value of 1. To check this behavior, we use the calculation geometry shown in Fig. 4. The nonhydrogen atom (X) is located on the contour around the collinear axis with the radius $q = 1.0$ bohr, while the distances between the hydrogen and nonhydrogen atoms along the collinear axis are fixed as follows: $r_{H-B} = 2.0$ bohr, $r_{H-N} = 1.95$ bohr, $r_{H-C} = 2.0$ bohr, and $r_{H-O} = 1.85$ bohr. In Table II, calculated results of x components of NAC of the previously discussed Renner-Teller systems by TDDFT using the d matrix are listed. In comparison with the CASSCF results [25], the signs are correctly obtained, and the magnitudes show reasonable agreement. The angular NAC, computed as the product of the contour radius q and the x component of NAC on the rotated X atom in Fig. 4 when $\varphi = 0$, is close to 1.0. This behavior is consistent with previous *ab initio* results of Renner-Teller systems [47,51,52]. In particular, the sum rule of NAC is shown to hold in TDDFT results of all cases, which has not been achieved for NH_2 and H_2O^+ in our previous TDDFT calculations using the h -matrix formula. Therefore, the PP

TABLE I. The x components of NAC (in bohr $^{-1}$) on three atoms of Li_3 and Na_3 trimers, which are at the geometry of Fig. 2 with $R_{Li-Li} = 5.0$ bohr and $R_{Na-Na} = 6.0$ bohr. The contour radius $q = 1.0$ bohr and angle $\varphi = 0$. Calculation results by the two TDDFT methods, using the h matrix and the d matrix, respectively, are compared.

		TDDFT (d matrix)	TDDFT (h matrix)
Li_3	Atom 1	-0.267	-0.303
	Atom 2	0.530	0.490
	Atom 3	-0.267	-0.303
Na_3	Atom 1	-0.351	-0.326
	Atom 2	0.699	0.583
	Atom 3	-0.351	-0.326

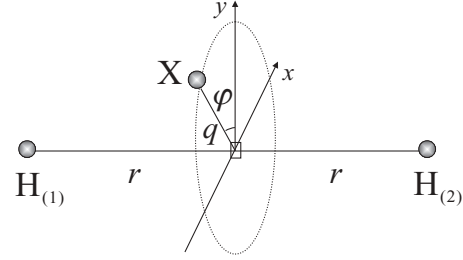


FIG. 4. Geometry of the XH_2 (or XH_2^+) system when the X atom is moved on the contour around the Renner-Teller intersection point (indicated by the open square) on the collinear axis. The contour, with radius q and angle φ , is fixed in the xy plane, which is perpendicular to the H-H axis. The two hydrogen atoms are set to be symmetric to the plane.

problem in evaluating h -matrix elements has been avoided when using the present d -matrix formulation.

B. Performance of the Slater transition-state method on computation of NAC in the very vicinity of Jahn-Teller and Renner-Teller intersections

For doublet systems, the application of the Slater transition-state method is justified as it gives equivalent results of NAC to TDDFT modified linear response theory. Many systems possessing Jahn-Teller or Renner-Teller intersections in the PES are known to be in doublet states; therefore, the Slater method is anticipated to give accurate NAC even in the very vicinity of intersection points. Work on this aspect has not been reported in the literature yet, although the performance of the Slater method on computing NAC of molecular systems in equilibrium geometries has been evaluated [27], where the values of NAC are quite small, compared with those very close to the intersection points.

1. Jahn-Teller systems

In Fig. 5 we show the x components on the second atom of H_3 in the hyperspherical coordinate (same configuration as in Fig. 1, that is, $\rho = 2.5$ bohr and $\phi = 120^\circ$) as a function of θ . Comparison with the reference data of MCSCF CI calculations [46] shows that the result is very encouraging: The data points are nearly in coincidence, not only in the region of θ larger than 1° but also even when θ is decreased to as small as 0.01° .

TABLE II. The x components of NAC (in bohr $^{-1}$) on three atoms of XH_2 ($X = B, N$) or XH_2^+ ($X = C, O$) molecules, which are at the geometry of Fig. 4. The contour radius q is taken as 1.0 bohr and angle φ is 0.

Method	Atom	BH_2	NH_2	CH_2^+	H_2O^+
TDDFT	$H_{(1)}$	-0.482	-0.495	-0.488	-0.502
	X	1.014	1.067	1.033	1.087
	$H_{(2)}$	-0.482	-0.495	-0.488	-0.502
CASSCF	$H_{(1)}$	-0.479	-0.475	-0.486	-0.485
	X	0.977	0.969	0.979	0.979
	$H_{(2)}$	-0.479	-0.475	-0.486	-0.485

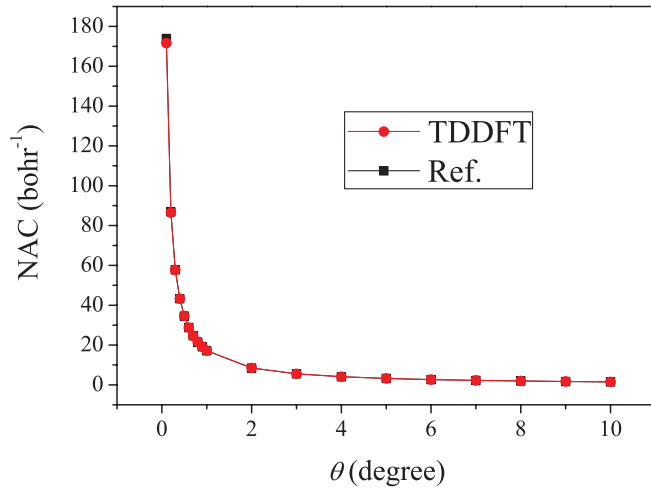


FIG. 5. (Color online) The x components of NAC on the second atom of H_3 as a function of the hyperspherical angle θ , computed by the Slater transition-state method (filled circles), to which modified linear response TDDFT calculations give equivalent results. The reference data (filled squares) are from MCSCF CI calculations by Abrol *et al.* [46].

Although our previous TDDFT calculation of NAC using the h matrix also shows that reasonable agreement can be achieved in the region of $\theta < 1^\circ$, such a good agreement had not been achieved and it hints that there is still room in constructing more accurate h -matrix elements from the PP's, even in the case of hydrogen which has no core electrons.

Further calculation examples of Jahn-Teller systems are alkali metal trimers (Li_3 and Na_3) [53–55], coinage metal trimers (Cu_3 and Ag_3) [56–58], and group V trimers (N_3 and P_3) [59,60]. Correlated wave-function calculations on NAC's near intersection points of these systems have not been carried out yet. In order to be comparable to the values of NAC from the Jahn-Teller model, we locate the trimers in the geometry of Fig. 2 and choose a sufficiently small contour radius q of 0.02 bohr. In such a configuration, the angular NAC, calculated as the product of the x component of NAC on the rotating atom and the contour radius q when the contour angle is 0, is expected to be equal to the quantized value of 0.5 in the Jahn-Teller model. We use the following internuclear distances for corresponding trimers: $R_{Li-Li} = 5.0$ bohr, $R_{Na-Na} = 6.0$ bohr, $R_{Cu-Cu} = 4.0$ bohr, $R_{Ag-Ag} = 5.0$ bohr, $R_{N-N} = 2.6$ bohr, and $R_{P-P} = 4.0$ bohr. For the coinage metal trimers, relativistic HGH PP's are used. In Table III we list the Cartesian components of NAC on three atoms of these trimers, calculated by the Slater transition-state method. From the x components of the rotating atom (that is, atom 2), the angular NAC's are found to be very close to the quantized value of 0.5. In the more detailed comparison with the Jahn-Teller model, it is seen that all components are quite similar to the ideal values. This had not been achieved in our previous TDDFT calculations using the h matrix, where the accuracy of results of N_3 and P_3 are degraded. Therefore, the present TDDFT method using the d matrix has avoided the PP problem in constructing h -matrix elements.

TABLE III. The calculated x , y and z components of NAC (in bohr^{-1}) on three atoms of Li_3 , Na_3 , Cu_3 , Ag_3 , N_3 , and P_3 trimers, which are at the geometry of Fig. 2. The contour radius q is 0.02 bohr and angle φ is 0. The ideal values from the Jahn-Teller model are also listed for comparison.

		x	y	z
Li_3	Atom 1	-12.50	-21.57	0.00
	Atom 2	24.99	0.00	0.00
	Atom 3	-12.50	21.57	0.00
Na_3	Atom 1	-12.96	-22.39	0.00
	Atom 2	25.91	0.00	0.00
	Atom 3	-13.96	22.39	0.00
Cu_3	Atom 1	-12.60	-21.72	0.00
	Atom 2	25.19	0.00	0.00
	Atom 3	-12.60	21.72	0.00
Ag_3	Atom 1	-12.74	-21.98	0.00
	Atom 2	25.45	0.00	0.00
	Atom 3	-12.74	21.98	0.00
N_3	Atom 1	-12.36	-21.42	0.00
	Atom 2	24.71	0.00	0.00
	Atom 3	-12.36	21.42	0.00
P_3	Atom 1	-12.43	-21.50	0.00
	Atom 2	24.86	0.00	0.00
	Atom 3	-12.44	21.50	0.00
Model	Atom 1	-12.50	-21.65	0.00
	Atom 2	25.00	0.00	0.00
	Atom 3	-12.50	21.65	0.00

2. Renner-Teller systems

Four typical Renner-Teller systems, BH_2 , NH_2 , CH_2^+ , and H_2O^+ molecules, are re-examined. In order to be comparable to the values of NAC from the Renner-Teller model, we use the geometry shown in Fig. 4 and choose a sufficiently small q of 0.1 bohr. In Table IV, we list the x components of NAC's on three atoms of these molecules, calculated by the Slater transition-state method. All the y and z components of NAC's are zero, consistent with the ideal values, while the nonzero, x , components of NAC's are in good agreement with those from the Renner-Teller model: The calculated angular NAC, that is, the product of the NAC component on atom X and the contour radius q , is equivalent to the quantized value of 1. The same level of accuracy is seen for either hydrogen or nonhydrogen atoms. Again, such an accuracy has not been achieved in previous TDDFT calculations using the h matrix,

TABLE IV. The x components of NAC (in bohr^{-1}), calculated by the Slater transition-state method, on three atoms of XH_2 ($X = B, N$) or XH_2^+ ($X = C, O$) molecules, which are at the geometry of Fig. 4. The contour radius q is taken as 0.1 bohr and angle φ is 0. The ideal values from the Renner-Teller model are also listed for comparison.

	BH_2	NH_2	CH_2^+	H_2O^+	Model
Atom $H_{(1)}$	-4.995	-5.000	-4.997	-5.001	-5.0
Atom X	9.994	10.001	10.000	10.001	10.0
Atom $H_{(2)}$	-4.995	-5.000	-4.997	-5.001	-5.0

showing that the present TDDFT scheme using the d matrix has avoided the PP problem.

V. CONCLUSION

We have studied the TDDFT density response scheme for computing NAC. Starting from the previous formulation where NAC is described using h -matrix elements, that is, matrix elements of $\partial H/\partial R_\mu$, an alternative description was provided using d -matrix elements, that is, matrix elements of $\partial/\partial R_\mu$. The new formulation has been shown to have an important advantage of eliminating the pseudopotential problem in the computation of NAC. The reason is that the new formulation avoids using the off-diagonal scattering terms, which is problematic within pseudopotential schemes. Evaluation of NAC near either the Jahn-Teller or the Renner-Teller intersection in various molecular systems validates this point and shows that the values of NAC are much improved over previous calculations when the d -operator formula is implemented in the pseudopotential framework. The new formulation has another advantage of allowing us to examine the previously proposed d -matrix-based formulation for NAC. When combined with

modified linear response theory it can justify the intuitive Slater transition-state method for doublet systems. This is important as many systems possessing Jahn-Teller or Renner-Teller intersections are known to be in doublet states. The new formulation also explains reasonably good performance of the Casida ansatz (the auxiliary wave-function ansatz) on the demonstrated systems in the literature, and shows an improved way of using the Casida ansatz for the general purpose of computing NAC. Finally, we would like to comment that the d -matrix formulation is sometimes numerically more time-consuming than the h -matrix formulation and that developing a pseudopotential to reproduce also the off-diagonal element will be the next target since the pseudopotential approach has shown promise in providing accurate data of NAC for the quantum simulation of nonadiabatic dynamics.

ACKNOWLEDGMENTS

This work was supported in part by Grant-in-Aid for Scientific Research (C) 20540384 and the Next Generation Super Computing Project, Nanoscience Program, MEXT, Japan.

-
- [1] H. A. Jahn and E. Teller, *Proc. R. Soc. Lond. A* **161**, 220 (1937).
 [2] S. Aronowitz, *Phys. Rev. A* **14**, 1319 (1976).
 [3] M. Baer, S. H. Lin, A. Alijah, S. Adhikari, and G. D. Billing, *Phys. Rev. A* **62**, 032506 (2000).
 [4] S. Adhikari, G. D. Billing, A. Alijah, S. H. Lin, and M. Baer, *Phys. Rev. A* **62**, 032507 (2000).
 [5] O. Butriy, H. Ebadi, P. L. de Boeij, R. van Leeuwen, and E. K. U. Gross, *Phys. Rev. A* **76**, 052514 (2007).
 [6] D. R. Yarkony, *Rev. Mod. Phys.* **68**, 985 (1996).
 [7] M. Baer, *Beyond Born-Oppenheimer: Electronic Nonadiabatic Coupling Terms and Conical Intersections* (Wiley, Hoboken, NJ, 2006).
 [8] E. Tapavicza, I. Tavernelli, and U. Rothlisberger, *Phys. Rev. Lett.* **98**, 023001 (2007).
 [9] E. Tapavicza, I. Tavernelli, U. Rothlisberger, C. Filippi, and M. E. Casida, *J. Chem. Phys.* **129**, 124108 (2008).
 [10] U. Werner, R. Mitrić, T. Suzuki, and V. Bonačić-Koutecký, *Chem. Phys.* **349**, 319 (2008).
 [11] H. Hirai and O. Sugino, *Phys. Chem. Chem. Phys.* **11**, 4570 (2009).
 [12] R. G. Sadygov and D. R. Yarkony, *J. Chem. Phys.* **109**, 20 (1998).
 [13] J. Neugebauer, E. J. Baerends, and M. Nooijen, *J. Chem. Phys.* **121**, 6155 (2004); *J. Phys. Chem. A* **109**, 1168 (2005).
 [14] X. Li, J. C. Tully, H. B. Schlegel, and M. J. Frisch, *J. Chem. Phys.* **123**, 084106 (2005).
 [15] C. M. Isborn, X. Li, and J. C. Tully, *J. Chem. Phys.* **126**, 134307 (2007).
 [16] V. Chernyak and S. Mukamel, *J. Chem. Phys.* **112**, 3572 (2000).
 [17] R. Baer, *Chem. Phys. Lett.* **364**, 75 (2002).
 [18] C. Hu, H. Hirai, and O. Sugino, *J. Chem. Phys.* **127**, 064103 (2007).
 [19] C. Hu, H. Hirai, and O. Sugino, *J. Chem. Phys.* **128**, 154111 (2008).
 [20] M. E. Casida, in *Recent Advances in Density Functional Methods, Part I*, edited by D. P. Chong (World Scientific, Singapore, 1995), p. 155.
 [21] C. Jamorski, M. E. Casida, and D. R. Salahub, *J. Chem. Phys.* **104**, 5134 (1996).
 [22] E. Renner, *Z. Phys.* **92**, 172 (1934).
 [23] C. Hu, O. Sugino, and Y. Miyamoto, *Phys. Rev. A* **74**, 032508 (2006).
 [24] C. Hu and O. Sugino, *J. Chem. Phys.* **126**, 074112 (2007).
 [25] C. Hu, O. Sugino, and Y. Tateyama, *J. Chem. Phys.* **131**, 114101 (2009).
 [26] M. Tommasini, V. Chernyak, and S. Mukamel, *Int. J. Quantum Chem.* **85**, 225 (2001).
 [27] S. R. Billeter and A. Curioni, *J. Chem. Phys.* **122**, 034105 (2005).
 [28] I. Tavernelli, E. Tapavicza, and U. Rothlisberger, *J. Mol. Struct. Theochem.* **914**, 22 (2009).
 [29] N. L. Doltsinis and D. S. Kosov, *J. Chem. Phys.* **122**, 144101 (2005).
 [30] C. F. Craig, W. R. Duncan, and O. V. Prezhdo, *Phys. Rev. Lett.* **95**, 163001 (2005).
 [31] W. R. Duncan, C. F. Craig, and O. V. Prezhdo, *J. Am. Chem. Soc.* **129**, 8528 (2007).
 [32] S. A. Fischer, W. R. Duncan, and O. V. Prezhdo, *J. Am. Chem. Soc.* **131**, 15483 (2009).
 [33] I. Tavernelli, B. F. E. Curchod, and U. Rothlisberger, *Phys. Rev. A* **81**, 052508 (2010).
 [34] M. Petersilka, U. J. Gossmann, and E. K. U. Gross, *Phys. Rev. Lett.* **76**, 1212 (1996).
 [35] M. Thiele and S. Kümmel, *Phys. Rev. A* **80**, 012514 (2009).
 [36] I. Tavernelli, B. F. E. Curchod, and U. Rothlisberger, *J. Chem. Phys.* **131**, 196101 (2009).
 [37] X. Gonze *et al.*, *Comput. Mater. Sci.* **25**, 478 (2002). The ABINIT code is a common project of the Université Catholique de

- Louvain, Corning Incorporated, the Université de Liège, Mitsubishi Chemical Corp., and other contributors (<http://www.abinit.org>).
- [38] S. Goedecker, M. Teter, and J. Hutter, *Phys. Rev. B* **54**, 1703 (1996).
- [39] N. Troullier and J. L. Martins, *Phys. Rev. B* **43**, 1993 (1991).
- [40] S. G. Louie, S. Froyen, and M. L. Cohen, *Phys. Rev. B* **26**, 1738 (1982).
- [41] C. Hartwigsen, S. Goedecker, and J. Hutter, *Phys. Rev. B* **58**, 3641 (1998).
- [42] I. Tavernelli, E. Tapavicza, and U. Rothlisberger, *J. Chem. Phys.* **130**, 124107 (2009).
- [43] A. J. C. Varandas, F. B. Brown, C. A. Mead, D. G. Truhlar, and N. C. Blais, *J. Chem. Phys.* **86**, 6258 (1987).
- [44] G. Halász, Á. Vibók, A. M. Mebel, and M. Baer, *Chem. Phys. Lett.* **358**, 163 (2002).
- [45] G. Halász, Á. Vibók, A. M. Mebel, and M. Baer, *J. Chem. Phys.* **118**, 3052 (2003).
- [46] R. Abrol, A. Shaw, and A. Kuppermann, *J. Chem. Phys.* **115**, 4640 (2001).
- [47] M. Desouter-Lecomte, D. Dehareng, B. Leyh-Nihant, M. Th. Praet, A. J. Lorquet, and J. C. Lorquet, *J. Phys. Chem.* **89**, 214 (1985).
- [48] I. B. Bersuker, *Chem. Rev.* **101**, 1067 (2001).
- [49] W. Reuter and S. D. Peyerimhoff, *Chem. Phys.* **160**, 11 (1992).
- [50] B. Engels and M. Perić, *J. Chem. Phys.* **97**, 7629 (1992).
- [51] G. J. Halász, Á. Vibók, R. Baer, and M. Baer, *J. Chem. Phys.* **124**, 081106 (2006).
- [52] G. J. Halász, Á. Vibók, D. K. Hoffman, D. J. Kouri, and M. Baer, *J. Chem. Phys.* **126**, 154309 (2007).
- [53] J. L. Martins, R. Car, and J. Buttet, *J. Chem. Phys.* **78**, 5646 (1983).
- [54] P. Soldán, M. T. Cvitas, and J. M. Hutson, *Phys. Rev. A* **67**, 054702 (2003).
- [55] P.-H. Zhang and J.-M. Li, *Phys. Rev. A* **54**, 665 (1996).
- [56] C. A. Mead, *Rev. Mod. Phys.* **64**, 51 (1992).
- [57] M. Kabir, A. Mookerjee, and A. K. Bhattacharya, *Phys. Rev. A* **69**, 043203 (2004).
- [58] Y. Shen and J. J. BelBruno, *J. Chem. Phys.* **118**, 9241 (2003).
- [59] J. N. Murrell, O. Novaro, S. Castillo, and V. Saunders, *Chem. Phys. Lett.* **90**, 421 (1982).
- [60] K. Balasubramanian, K. Sumathi, and D. Dai, *J. Chem. Phys.* **95**, 3494 (1991).